

EFFECTS OF STERILIZATION ON SHAPE MEMORY POLYURETHANE  
EMBOLIC FOAM DEVICES

A Thesis

by

RACHAEL LEE MUSCHALEK

Submitted to the Office of Graduate and Professional Studies of  
Texas A&M University  
in partial fulfillment of the requirements for the degree of

MASTER OF SCIENCE

Chair of Committee,	Duncan J. Maitland
Committee Members,	Balakrishna Haridas
	Suresh Pillai
Head of Department,	Anthony Guiseppi-Elie

May 2017

Major Subject: Biomedical Engineering

Copyright 2017 Rachael L. Muschalek

## ABSTRACT

Shape memory polymer (SMP) foams have been developed for various embolic applications. These polyurethane materials can be deformed and stored in a secondary shape, from which they can recover their primary shape after exposure to an external stimulus, such as heat and moisture. Tailored actuation temperatures of SMPs provide benefits for minimally invasive biomedical applications, but incur significant challenges for SMP-based medical device sterilization. Most sterilization methods require high temperature and/or humidity to effectively reduce the bioburden of the device, but the environment must be tightly controlled after device fabrication.

Here, three probable sterilization methods: non-traditional ethylene oxide (ntEtO) gas sterilization gamma irradiation, and electron beam (ebeam) irradiation were investigated for SMP-based embolic medical devices. SMP foam was tested for changes in thermal properties using differential scanning calorimetry. Mechanical testing was used to analyze sterilization-induced material changes. Unconstrained expansion profiles were obtained to see if sterilization affected the shape memory properties of the foam. Finally, spectroscopy was done to analyze potential molecular changes in the foams.

Thermal characterization of the sterilized foams indicated that ntEtO gas sterilization decreased the glass transition temperature. Gamma irradiation was hypothesized to generate oxidative radicals that threaten the biostability of the

embolic medical device. Further material characterization was undertaken on the ebeam sterilized samples, which indicated minimal changes to foam integrity and device functionality.

## DEDICATION

To my parents, who have supported me from the beginning to follow my dreams no matter where they might lead me. Thank you, mom, for continually reminding me that life should be fun and to not take anyone or anything too seriously. To my father, who answered all of my unending questions as a child and continued to push me to think critically about the world around me as an adult. I wouldn't be who I am today without your unending love and support. I love you both so much.

## ACKNOWLEDGEMENTS

I would like to thank my committee chair, Dr. Duncan Maitland, for believing in me as a student and researcher as early as my sophomore year. Dr. Maitland supported me through many years of academic endeavors and has helped to shape my future more than he will ever know. He was patient with my many mistakes along the way and gave me so much more than a Master's degree. He pushed me to pursue the career that excited me and he made all of my dreams not only possible, but also plausible because of his help. He taught me that it isn't making a mistake that causes a failure but how you handle your mistakes. Thank you for believing in me and pushing me to be the best student and researcher I could be.

Thanks also to my committee members, Dr. Haridas, and Dr. Pillai for their guidance and support throughout the course of this research. I sincerely appreciate all of their helpful feedback I have received and I wouldn't have been able to complete this work without them.

I would also like to thank Dr. Mary Beth Monroe for teaching me how to be an effective writer and always being such a positive influence on my writing ability. She was so patient with my many reviews and was so eager to help with any problems or issues I had.

Thank you to Dr. Marziya Hasan and Dr. Landon Nash for their unending support in the research lab and for answering my incessant questions about research,

writing, graduating, professional development, and just general life. You both helped shape me to be the researcher and student that I am.

I would like to thank the rest of the BDL for being such a supportive academic environment. I enjoyed my time with each and every one of you. I will miss our nerf wars in the office and our weekend game nights. You all made graduate school worth it.

Lastly, I would like to thank Mr. Kevin Korpi and Mr. Trent Wenzel of New Braunfels High School. You both ignited in me a passion for science, math, and critical thinking that extended well beyond the walls of NBHS. You helped shape my life path and always reminded me to have fun in whatever I was doing.

## CONTRIBUTORS AND FUNDING SOURCES

This work was supported by a thesis committee consisting of Professor Duncan Maitland (advisor) and Professor Balakrishna Haridas of the Department of Biomedical Engineering and Professor Suresh Pillai of Department of Poultry Science.

All electron beam samples were irradiated at the National Center for Electron Beam Research on Texas A&M's campus with the assistance of Mickey Speakmon and Emma Link.

Graduate study was supported by a Merit Fellowship from Texas A&M University, an Enrichment Fellowship from the Department of Biomedical Engineering, and Teaching Assistantships in the Department of Biomedical Engineering.

## NOMENCLATURE

SMP	Shape memory polymer
T <sub>trans</sub>	Transition temperature
SME	Shape memory effect
T <sub>m</sub>	Melt transition temperature
T <sub>g</sub>	Glass transition temperature
BDL	Biomedical Device Lab
NED	Neurovascular embolization device
Nitinol	Nickel-titanium alloy
PED	Peripheral embolization device
AVM	Arteriovenous malformations
ntEtO	Non-traditional ethylene oxide
Ebeam	Electron beam radiation
EtO	Ethylene Oxide
HPED	N,N,N',N'-tetrakis(2-hydroxypropyl)ethylenediamine
TEA	Triethanolamine
TMHDI	Trimethyl-1,6-hexamethylene diisocyanate
HDI	Hexamethylene diisocyanate
IPA	2-propanol
DI	Deionized water
NCO	Isocyanate



OH	Hydroxyl
RO	Reverse Osmosis
DSC	Differential scanning calorimetry
UTS	Ultimate tensile stress
FTIR	Fourier transform infrared spectroscopy
DMA	Dynamic mechanical analysis
ATR	Attenuated total reflectance

## TABLE OF CONTENTS

	Page
ABSTRACT .....	ii
DEDICATION .....	iii
ACKNOWLEDGEMENTS .....	iv
CONTRIBUTORS AND FUNDING SOURCES.....	vi
NOMENCLATURE.....	vii
TABLE OF CONTENTS .....	ix
LIST OF FIGURES.....	xi
LIST OF TABLES .....	xiii
CHAPTER I INTRODUCTION .....	1
1.1 Shape memory polymer foams.....	1
1.2 Neurovascular embolization for treatment of intracranial aneurysms .....	4
1.3 Peripheral embolization device for various malformations .....	6
1.4 Sterilization of SMP foams .....	7
1.5 Summary of thesis.....	11
CHAPTER II METHODS AND MATERIALS .....	12
2.1 Materials.....	12
2.2 Foam synthesis .....	12
2.3 Cleaning .....	13
2.4 Packaging .....	14
2.5 Sterilization .....	14
2.6 Characterization.....	15
CHAPTER III RESULTS .....	18
3.1 Results .....	18
3.2 Differential scanning calorimetry (DSC) .....	18
3.3 Mechanical testing.....	19

3.4 Crimp diameter.....	21
3.5 Unconstrained expansions.....	22
3.6 Fourier transform infrared (FTIR) spectroscopy.....	25
CHAPTER IV DISCUSSION AND CONCLUSIONS .....	27
4.1 Summary .....	27
4.2 Discussion .....	28
4.3 Challenges and future work.....	30
REFERENCES.....	32

## LIST OF FIGURES

	Page
Figure 1.1: Shape memory effect (SME) of a thermally actuated SMP. SMPs can be fixed into a secondary shape by heating above its $T_{trans}$ and applying a mechanical force to deform the polymer into the desired secondary shape. Cooling the polymer below its $T_{trans}$ while maintaining the mechanical deformation will set the secondary shape. Upon heating the SMP above its $T_{trans}$ , the polymer will recover to its primary shape. ....	2
Figure 1.2: SME for an amorphous polymer system. The $T_{trans}$ for this system is the $T_g$ of the SMP. The netpoints of the amorphous polymer will determine the primary shape, while the switching segments allow for the SME. Reprinted with permission from Lendlein et. al. [1]. ....	3
Figure 1.3: Currently available treatments for cerebral aneurysms and the proposed SMP device. A) Surgical clipping, B) Endovascular coiling, and C) SMP foam device that expands upon implantation and acts as a scaffold for cellular infiltration.....	5
Figure 1.4: Peripheral embolization device (PED) for occlusion of morbidities in the peripheral vasculature. Devices contain a platinum/ iridium alloy marker band and anchor coil for visualization and a SMP foam for rapid and complete vessel occlusion. Reprinted with permissions from Landsman et. al. [2] .....	7
Figure 1.5: A) Molecular example of hydrogen bonding between two polyurethane backbones B) Effects of moisture plasticization on polymer modulus versus temperature curve.....	8
Figure 3.1: $T_g$ measurements for the two foam compositions (A and B: 100TMH60; C and D: 100HDIH40) in wet (A and C) and dry (B and D) conditions. N = 3, average $\pm$ standard deviation displayed. ....	20
Figure 3.2: UTS of a) 100TMH60 and b) 100HDIH40 foams. No significant changes were seen before and after sterilization. N = 6, average $\pm$ standard deviation displayed. ....	21
Figure 3.3: Strain at break of a) 100TMH60 and b) 100HDIH40 foams. No significant changes were seen before and after sterilization. N = 6, average $\pm$ standard deviation displayed.....	21

Figure 3.4: Cylindrically crimped 1 mm 100TMH60 foam after each method of sterilization. Images were taken with a Jenoptic microscope camera and analyzed using ImageJ software for average diameter.....22

Figure 3.5: Unconstrained expansion over time of exposure to 37°C water for ebeam-sterilized (a) 100TMH60, (b) 100HDIH40, and (c) 100HDIH60 foams. N = 3, average ± standard deviation displayed. Dotted line indicates initial cut diameter dimensions.....25

Figure 3.6: FTIR spectra of (a) 100TMH60, (b) 100HDIH40, and (c) 100HDIH60 before and after ebeam sterilization. ....27

## LIST OF TABLES

	Page
Table 2.1: Monomer ratios used in foam synthesis and final cylindrical device diameters used in testing (based on foam compositions required for each device prototype) .....	13
Table 3.1: Cylindrical expansion of 100TMH60 foams following sterilization. N = 7, average $\pm$ standard deviation displayed. ....	23
Table 3.2: Cylindrical expansion of 100HDIH40 foams following sterilization. N = 3, average $\pm$ standard deviation displayed. ....	23

CHAPTER I  
INTRODUCTION<sup>1</sup>

**1.1. Shape memory polymer (SMP) foams**

Recent advances in material science have increased the use of polymers for biomedical applications [1] [3]. Stimuli responsive polymers, such as shape memory polymers (SMPs), have shown promise in polymer-based medical devices, including thrombus removal devices, cardiac valve repair devices, and various embolic devices[1] [4] [5] [6] [7]. SMPs are a class of smart material that are capable of being deformed and stored in a stable secondary shape and recovering to a primary form when exposed to a stimulus, such as heat (**Figure 1.1**) [4] [5] [8] [9]. Thermal SMPs are synthesized into their primary shape, which is fixed by crosslinking. The secondary shape is set *via* polymer deformation above its  $T_{trans}$ , and subsequent cooling back to its glassy state (below  $T_{trans}$ ) while maintaining the deformation [1]. Upon supplying sufficient thermal energy to the polymer system, entropic potential drives the shape recovery of the polymer from its secondary state to its primary shape [1].

---

<sup>1</sup> Parts of this chapter are from “Effects of Sterilization on Shape Memory Polyurethane Embolic Foam Devices” by **R. Muschalek**, Nash L.D., Jones R, Hasan S.M., Keller B.K., Monroe M.B., Maitland D.J., which is under review by the Journal of Medical Devices.

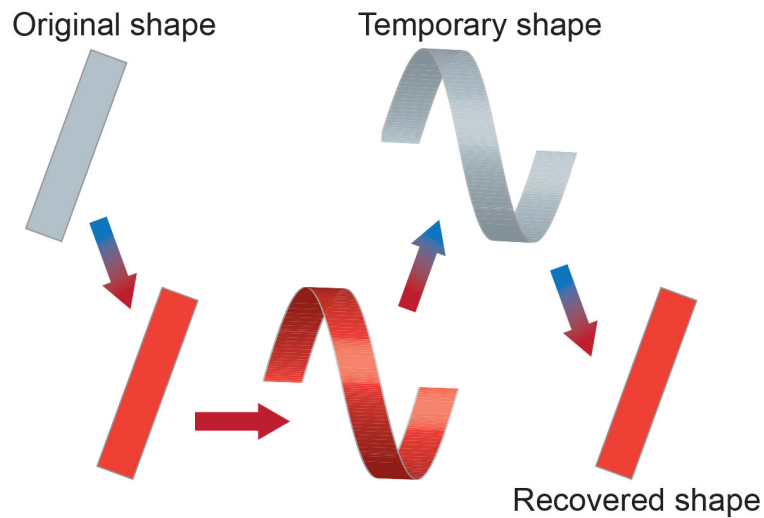


**Figure 1.1: Shape memory effect (SME) of a thermally actuated SMP. SMPs can be fixed into a secondary shape by heating above its  $T_{trans}$  and applying a mechanical force to deform the polymer into the desired secondary shape. Cooling the polymer below its  $T_{trans}$  while maintaining the mechanical deformation will set the secondary shape. Upon heating the SMP above its  $T_{trans}$ , the polymer will recover to its primary shape.**

SMPs are networks of switching segments and net points, where the net points determine the primary shape of the polymer and the switching segments allow deformation above  $T_{trans}$  by absorbing stress on the system. Predominantly crystalline SMPs have a  $T_{trans}$  equal to their melt transition temperature ( $T_m$ ), and predominantly amorphous materials exhibit a  $T_{trans}$  equivalent to their glass transition temperature ( $T_g$ ) [1].



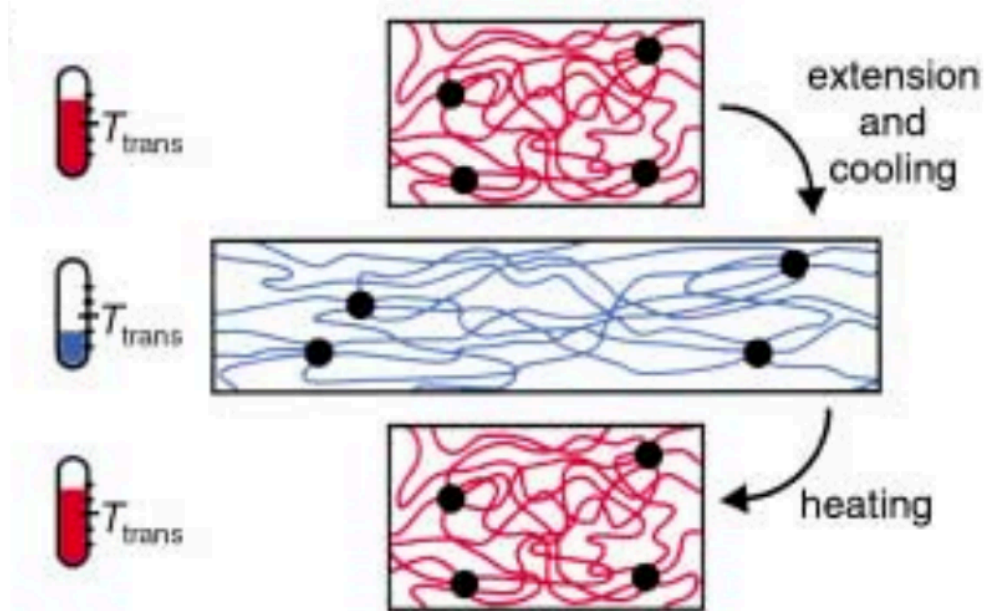


Figure 1.2: SME for an amorphous polymer system. The  $T_{\text{trans}}$  for this system is the  $T_g$  of the SMP. The netpoints of the amorphous polymer will determine the primary shape, while the switching segments allow for the SME. Reprinted with permission from Lendlein et. al. [1].

The SMPs used in this work are polyurethane SMP foams, which are synthesized as highly crosslinked amorphous polymers (**Figure 1.2**). This shape memory property allows for non-invasive or minimally-invasive implantable medical devices, as SMPs can be stored in a compressed form during delivery through a catheter, after which they expand to their primary shape upon heating to body temperature [4, 8, 9] [10] [11]. Additionally, these polymers are highly biocompatible, highly thrombogenic, exhibit tunable glass transition temperatures ( $-100\text{ }^{\circ}\text{C}$  to  $80\text{ }^{\circ}\text{C}$ ), ultra low densities ( $0.008\text{ g/cm}^3$ ), high porosities (98%), and X-ray visibility, which makes them ideal candidates for a wide range of medical devices, including aneurysm treatment [5] [9] [12] [13] [14].

An aneurysm is a weakening of the vascular wall that allows localized dilation and ballooning of the artery [15]. Aneurysms may be congenital or caused by defects in the vascular wall, such as atherosclerotic plaques [15] [16]. Additional risk factors, including hypertension and connective tissue disorders, have also been identified.

Aneurysms may occur in many sites in the body, but are most commonly found in the peripheral vasculature (including the aorta, mesenteric arteries and splenic arteries) or cerebral arteries. Aneurysms are susceptible to rupturing due to wall thinning, which causes a subarachnoid hemorrhage (SAH) if aneurysm is located intracranially or internal bleeding if aneurysm is located peripherally. The Biomedical Device Lab (BDL) at Texas A&M has developed two shape memory polyurethane embolic foam devices for treatment of both intracranial aneurysms and occlusion of the peripheral vasculature for various malformations.

## **1.2. Neurovascular embolization for treatment of intracranial aneurysms**

Most neurovascular aneurysms are spherical outpouchings, or saccular aneurysms, that range from 2-50 mm in diameter, with an average of 8 mm [17]. They are most commonly observed at the apex of the subarachnoid arterial bifurcations [18].

It is estimated that 30,000 intracranial aneurysms rupture in the United States every year, and approximately 3-5 million Americans have or will develop an intracranial saccular aneurysm in their lifetime [15] [19]. If an aneurysm ruptures to cause a SAH, there is a reduction in cerebral blood flow, reduced cerebral autoregulation, an increase in intracranial pressure, and acute vasoconstriction, all of

which pose significant danger to the viability of the cerebral tissue [20]. It is estimated that only half of patients will survive a SAH, and there is substantial morbidity among survivors [20]. Currently available treatments for intracranial aneurysms include surgical clipping and endovascular coiling, as well as the proposed device from the BDL (Figure 1.3 A-C).

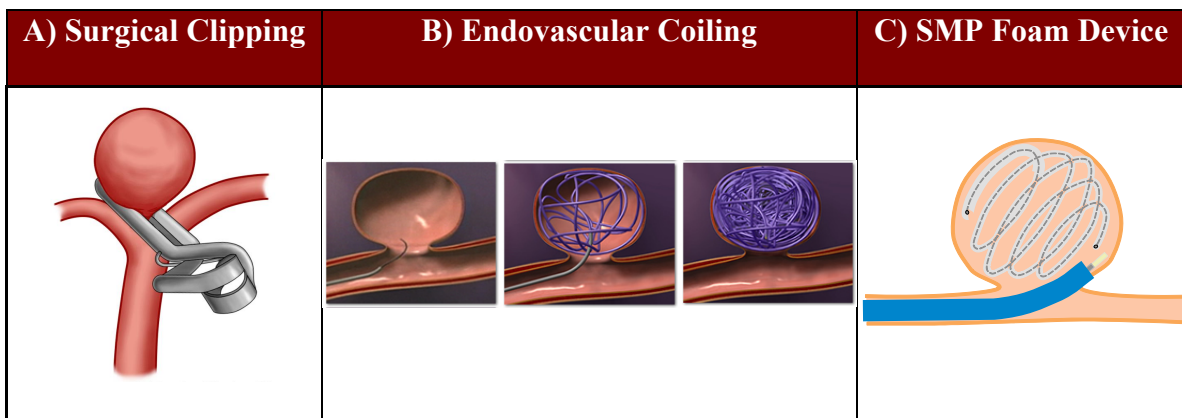


**Figure 1.3: Currently available treatments for cerebral aneurysms and the proposed SMP device. A) Surgical clipping [21], B) Endovascular coiling [22], and C) SMP foam device that expands upon implantation and acts as a scaffold for cellular infiltration**

Aneurysm clipping requires a high-risk, invasive surgery to implant a metal clip at the base of the aneurysm to prevent blood flow into the aneurysm sac and close off the aneurysm neck (Figure 1.3 A) [23]. Depending on the aneurysm location, size and neck geometry, a surgeon may not be able to safely clip the aneurysm [24]. Additionally, as with any invasive procedure, there is a longer recovery time and the possibility of infection [24].

Endovascular coiling (Figure 1.3 B) provides a minimally invasive approach to aneurysm treatment that aims to fill the aneurysm sac with materials (primarily soft

platinum coils) to reduce the risk of rupture or re-bleeding [24]. This approach allows for better access to the tortuous vasculature, because coils are delivered through a microcatheter to the aneurysm sac with the aid of fluoroscopy imaging [25]. However, a ten-year retrospective review of aneurysm coiling patients found that 24.5% of patients experienced recanalization and approximately 5% required additional treatment [25]. In addition to high rates of recanalization, these devices are also plagued by chronic inflammation [26] and low occlusion rates (23-37%) [27] [28]. Polymer coated coils were introduced to address some of these issues, which showed promising results initially; however, as the polymer was resorbed by the body, recanalization occurred [29].

Polyurethane SMP foams have been incorporated into a neurovascular embolization device (NED) and have shown excellent embolic and healing responses [14] [30] (**Figure 1.3 C**). The SMP foam is threaded over a core of platinum wound nickel-titanium (nitinol) [11], which makes these devices well suited for clinical adoption due to the similarity to existing devices. SMP devices passively actuate at body temperature (37°C), can be delivered non-invasively through a microcatheter, and detach *via* a similar mechanism to current coil devices [31].

### **1.3 Peripheral embolization device (PED) for various malformations**

In certain conditions, physicians utilize embolization devices to divert blood flow from a region outside the vasculature of the brain. As with cerebral aneurysms, embolization is a technique that is often utilized instead of an invasive surgery to block

blood flow to specific anatomies. This treatment can be used to address a variety of morbidities, such as arteriovenous malformations (AVM), venous insufficiency, patent foramen ovals, or traumatic internal bleeding [32] Polyurethane SMP foams show promise for complete occlusion with a single device for any of the aforementioned conditions [4, 33] [32]. SMP-based PEDs also contain a platinum/ iridium alloy anchor coil and marker band for device visualization under fluoroscopy [32].

### **Impede™ Peripheral Embolization Device**

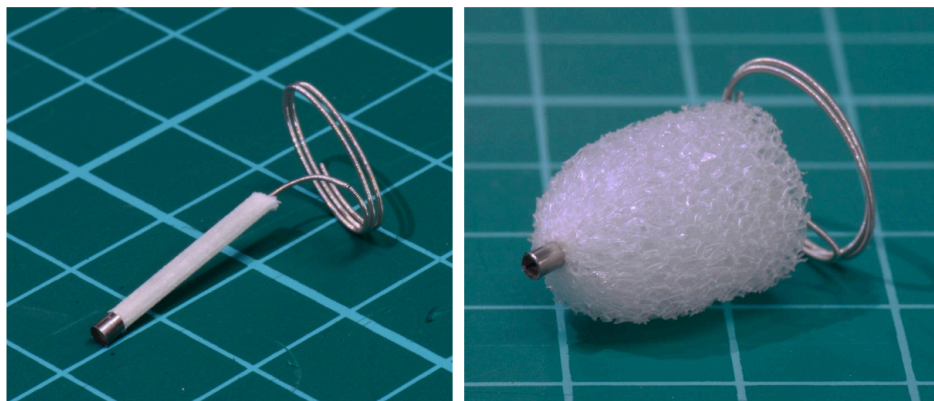


**Figure 1.4: PED for occlusion of various morbidities in the peripheral vasculature. Devices contain a platinum/ iridium alloy marker band and anchor coil for visualization and SMP foam for rapid and complete vessel occlusion. Reprinted with permissions from Landsman et. al. [2]**

#### **1.4 Sterilization of SMP foams**

Preliminary efforts have focused on device fabrication and functionality [11] [10], but other hurdles must be overcome to realize the clinical potential of these SMP-based devices; namely, a validated sterilization method is required to gain regulatory approval [34] [35] [36] [37] [38] [39].

The proposed thermoset polyurethanes have excellent shape memory capacity due to their extensive crosslinking [40], but chain-chain hydrogen bonding influences the temperature at which these polymers actuate (**Figure 1.5 A**). Disruption of this hydrogen-bonding network can occur *via* plasticizers, the most common of which is water [8]. In the case of stimuli-responsive polymers, plasticization can drastically reduce the actuation temperature at which shape recovery occurs [8] (**Figure 1.5 B**). The shape memory property of these foams is dependent upon a combination of moisture plasticization and thermal actuation from heating to body temperature [8] [10] [11]. Premature actuation could lead to the polymer system expanding within the delivery catheter and subsequent failure of the medical device [8] [10] [11]. Thus, a major hurdle for medical device approval is sterilization of this heat and moisture sensitive polymer system while minimizing the chance of premature actuation.

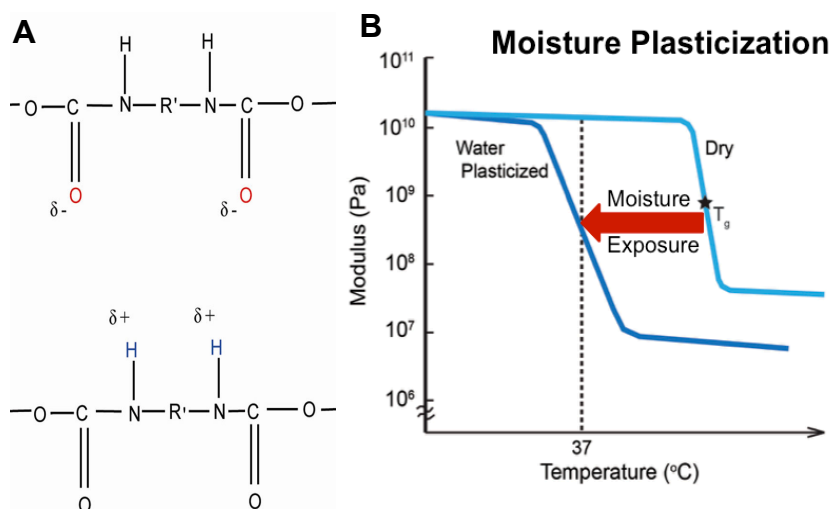


**Figure 1.5:** A) Molecular example of hydrogen bonding between two polyurethane backbones B) Effect of moisture plasticization on polymer modulus versus temperature

There are a number of methods available for sterilization of an implantable medical device [35] [41] [42] [43]. This research explores three potential sterilization methods for the polyurethane SMP embolic foams: non-traditional ethylene oxide (ntEtO) gas sterilization [11], gamma beam irradiation, and electron beam irradiation (ebeam).

### *1.3.1 Non-Traditional Ethylene Oxide*

Ethylene oxide (EtO) gas sterilization requires gaseous diffusion into the packaging in order for the bactericidal, sporicidal, and virucidal gas to interact with the microbes on the device [43]. Packaging with gas permeable films segments, such as foil header pouches, is necessary for effective EtO sterilization. These gas permeable segments, or headers, enable gas and moisture diffusion into the pouch for effective sterilization and subsequent EtO off-gassing. Moisture is important for effectively killing desiccated bacterial spores during sterilization, and residual EtO must be effectively removed prior to device implantation [43]. EtO gas is highly flammable and potentially hazardous for patients and sterilization handlers [41]. For safety reasons, porous materials are required to aerate for at least 48 hours after EtO sterilization [43]. NtEtO differs from EtO sterilization in that it has lower heat and humidity requirements to achieve sterility.

### *1.3.2 Gamma Beam Irradiation*

Gamma beam irradiation sterilizes medical devices by penetrating packaging and destroying the covalent bonds of DNA strands and other important biomolecules [44]. The primary source of gamma rays is cobalt 60, which emits gamma rays during decay and is generally considered a cold method (no increase in temperature is required) [44] [45]. Gamma radiation is a safe, reliable method of sterilization but has been shown to enhance material degradation and therefore may not be useful for some polymer-based medical devices [42] [45] [46] . Due to the generation of oxidative radicals during ionization that can potentially lead to material degradation, the packaging plays a crucial role in post-sterilization material properties.

### *1.3.3 Electron Beam Irradiation*

Ebeam radiation uses an electron linear accelerator to shower devices with ionizing radiation to sterilize the devices in a similar manner to gamma radiation but with a quicker turnaround time [47]. Ebeam requires less exposure time due to the higher dosing rate, leading to reduced potential polymer degradation [46]. Increased available energy, improved reliability, and absence of a source that steadily depletes over time are additional advantages to the use of ebeam sterilization [45]. A major limitation of ebeam sterilization is its reduced penetration and density-dependent gradient within the medical device [46]. Nitrogen purged, vacuum-sealed foil pouches are used to limit oxygen and moisture diffusion in the packaging that could cause polymer oxidation during irradiation.



## **1.5 Summary of thesis**

A validated sterilization method is required for clinical translation of both the neurovascular aneurysm occlusion device as well as the Impede <sup>TM</sup> peripheral occlusion device. The goal of this thesis is to explore the material characteristics of SMP foams and foam devices before and after sterilization and make a final recommendation for a sterilization method to be used in commercialization.

Chapter II discusses the materials and methods of SMP foam synthesis and characterization that were undertaken. Sterilized foam samples were characterized using tensile testing, differential scanning calorimetry, unconstrained cylindrical expansion, and Fourier transform infrared (FTIR) spectroscopy. The methods of analysis are presented.

Chapter III presents the results from material characterization before and after sterilization. This work was done in an effort to assess the effects of three aforementioned sterilization methods on final device performance.

Chapter IV provides a brief summary of results as well as a discussion of future works. A final recommendation for a sterilization method for device commercialization is given.

## CHAPTER II

### METHODS AND MATERIALS<sup>2</sup>

#### 2.1 Materials

N,N,N',N'-tetrakis(2-hydroxypropyl)ethylenediamine (HPED, 99%; Sigma-Aldrich Inc., St. Louis, MO), triethanolamine (TEA, 98%; Sigma-Aldrich Inc., St. Louis, MO), trimethyl-1,6-hexamethylene diisocyanate, 2,2,4- and 2,4,4-mixture (TMHDI; TCI America Inc., Portland, OR), hexamethylene diisocyanate (HDI; TCI America Inc., Portland, OR), DC 198 (Air Products and Chemicals Inc., Allentown, PA), DC 5943 (Air Products and Chemicals Inc., Allentown, PA), T-131 (Air Products and Chemicals Inc., Allentown, PA), BL-22 (Air Products and Chemicals Inc., Allentown, PA), Enovate 245fa Blowing Agent (Honeywell International Inc., Houston, TX), 2-propanol 99% (IPA) (VWR, Radnor, PA) and deionized (DI) water (E-Pure water system, Barnstead International, Dubuque, IA) were used as received.

#### 2.2 Foam Synthesis

Three different SMP foam formulations, shown in **Table 2.1**, were synthesized using the three-step protocol previously described by Hasan et al. [48, 49]. Briefly, isocyanate (NCO) pre-polymers were synthesized using appropriate molar ratios of HPED, TEA, TMHDI, and HDI, with a 35 wt % hydroxyl (OH) composition. A OH

---

<sup>2</sup> Parts of this chapter are from “Effects of Sterilization on Shape Memory Polyurethane Embolic Foam Devices” by **R. Muschalek**, Nash L.D., Jones R, Hasan S.M., Keller B.K., Monroe M.B., Maitland D.J., which is under review by the Journal of Medical Devices.

mixture was prepared with the remaining molar equivalents of HPED and TEA, along with catalysts, surfactants, and DI water. During foam blowing, a physical blowing agent, Enovate, was mixed with the isocyanate pre-polymer and the OH mixture using a speed-mixer (FlakTek Inc., Hauschild, Germany). The resulting foams were cured in a vacuum oven (Cascade Tek, Hillsboro, Oregon) at 90 °C for 20 minutes. The SMP foams were cooled to room temperature ( $21 \pm 1$  °C) followed by a 24-hour cold cure ( $21 \pm 1$  °C) before further processing.

**Table 2.1: Monomer ratios used in foam synthesis and final cylindrical device diameters used in testing (based on foam compositions required for each device prototype)**

<b>Formulation Name</b>	<b>Isocyanate (NCO)</b>	<b>HPED (molar eq.)</b>	<b>TEA (molar eq.)</b>	<b>Cylindrical Diameter (mm)</b>
<b>100TMH60</b>	TMHDI	60	40	1
<b>100HDIH40</b>	HDI	40	60	8
<b>100HDIH60</b>	HDI	60	40	6

### 2.3 Cleaning

Foams were cut into 2 mm slices using a resistively-heated wire cutter (Proxxon Thermocut, Prox-Tech Inc., Hickory, NC). The foam slices were shaped using a calibrated and certified ASTM Die D- 638 Type IV dog bone punch (Pioneer-Dietecs Corporation, Weymouth MA). Samples were then submerged in 1000 mL jars filled with IPA and sonicated for 2 x 15 minutes, refreshing the IPA between cycles. Reverse

osmosis (RO) water was used as a final wash for 15 minutes under sonication. Samples were removed, allowed to air dry, and then dried at 100 °C under vacuum for 12 hours.

## **2.4 Packaging**

Samples designated for sterilization were packaged in various sizes of foil header pouches (Tyvek Foil Pouches, Beacon Converters, Saddle Brooke NJ) using an AVN packaging system (AmeriVacS, San Diego, CA). Pouches were purged with nitrogen prior to vacuum sealing with heat. Included in all packages were a temperature indicator (S-6710 Telatemp Heat Indicator, Uline, Pleasant Prairie, WI) and a humidity indicator (S-8028 10 - 60% Humidity Indicator, Uline, Pleasant Prairie, WI). Dog bone SMP samples were secured inside the package using adhesive and wire. Cylindrical samples were attached with adhesive on each end. Samples designated for gas-based sterilization were sealed above a header that allowed gaseous exchange during sterilization and degassing. The headers were then sealed and removed to limit further moisture diffusion. Samples designated for radiation-based sterilization were completely vacuum-sealed within the foil portion of the pouch to prevent ambient oxygen from entering the pouch.

It should be noted that gamma radiation samples were packaged prior to receipt of the AVN packaging system and were not nitrogen purged or vacuum-sealed. This discrepancy may have had an impact on the results found and is noted in the discussion.

## 2.5 Sterilization

The ntEtO samples were sterilized with  $10.5 \text{ g} \pm 5\%$  of EtO gas with ambient humidity at  $30 \text{ }^\circ\text{C}$  for at least 12 hours at Andersen Scientific (Morrisville, NC). A biological indicator strip was placed inside the chamber by Anderson Scientific to ensure sterility of the ntEtO samples. Gamma radiation dog bone samples received 40 kGy (25 kGy + Safety Factor of 1.6) at a Sterigenics sterilization facility [36] [42]. Ebeam radiation samples received 40 kGy (25 kGy + Safety Factor of 1.6) at the National Center for Electron Beam Research (College Station, TX). A second series of ebeam testing was undertaken at 25 kGy [37].

## 2.6 Characterization

### 2.6.1 Differential scanning calorimetry (DSC)

Foam samples (2-6 mg) were used for glass transition temperature ( $T_g$ ) analysis using a Q-200 dynamic scanning calorimeter (DSC) (TA Instruments, Inc. New Castle, DE) to obtain wet and dry thermograms for the foams. Dry samples were stored in a desiccated container and hermetically sealed into aluminum pans. The first cycle consisted of decreasing the temperature to  $-40 \text{ }^\circ\text{C}$  at  $10 \text{ }^\circ\text{C}\cdot\text{min}^{-1}$  and holding it isothermally for 2 minutes. The temperature was then increased to  $120 \text{ }^\circ\text{C}$  at  $10 \text{ }^\circ\text{C}\cdot\text{min}^{-1}$  and held isothermally for 2 minutes. In the second cycle, the temperature was reduced to  $-40 \text{ }^\circ\text{C}$  at  $10 \text{ }^\circ\text{C}\cdot\text{min}^{-1}$ , held isothermally for 2 minutes, and raised to  $120 \text{ }^\circ\text{C}$  at  $10 \text{ }^\circ\text{C}\cdot\text{min}^{-1}$ .  $T_g$  was recorded from the second cycle based on the inflection point of the

thermal transition curve using TA instruments software. The aluminum tins were vented during this process. Each dry composition was measured at least three times.

Wet samples were prepared by allowing small foam samples to plasticize in 50 °C RO water for at least 10 minutes. Water was then pressed out using a mechanical press, and samples were tested on a cycle that decreased the temperature to -40 °C at 10 °C·min<sup>-1</sup> and holding it isothermally for 2 minutes. The temperature was then increased to 80 °C at 10 °C·min<sup>-1</sup>. Tg was recorded from the heating cycle as the inflection point on the thermal transition curve. Each wet composition was measured at least three times.

### *2.6.2 Mechanical testing*

Each end of the dog bone foam samples was attached to mechanical testing wooden stubs using clear epoxy adhesive and allowed to dry overnight under vacuum. Samples were then strained to failure using an Insight 30 material tester (Materials Testing Solutions, MTS Systems Corporation, Eden Prairie, MN). Stress versus strain curves were analyzed for ultimate tensile stress (UTS) and % strain at break. Each composition was tested at least six times.

### *2.6.3 Crimp diameter*

Foam cylinders (1-8 mm in diameter) were crimped around a nitinol backbone wire. Diameters for each foam cylinder were chosen according to clinical applicability (**Table 2.1**). Samples were placed inside the heated chamber of a stent crimper (100 °C) (Machine Solutions Inc., Flagstaff, AZ) and allowed to equilibrate for 10 minutes.

Crimpers were closed and cooled using room temperature air. Images were taken on a Jenoptik Microscope Camera (Jenoptik, Jena, Germany) 24 hours after crimping to generate a baseline of device diameter prior to sterilization. ImageJ (NIH, Bethesda, MD) processing software was used to quantify the device diameters prior to sterilization. Upon receipt of devices after nEtO and ebeam sterilization, images were taken again, and device diameter was re-measured. Any device expansion due to plasticization or process-related heating was noted. Each composition was measured at least three times.

#### *2.6.4 Unconstrained expansions*

Unconstrained expansion of cylindrical samples was assessed in a hot water bath to obtain actuation profiles after nEtO and ebeam sterilization. Devices were placed on a fixture and submerged in a 37 °C hot water bath. Images were taken with a digital camera (PowerShot SX230 HS, Canon Inc., Tokyo, Japan) every thirty seconds for 15 minutes and analyzed with ImageJ processing software to quantify device diameter over time. Each composition was measured three times.

#### *2.6.5 Fourier transform infrared (FTIR) spectroscopy*

Before and after ebeam irradiations, foam samples were cut to 2-3 mm thick, and the FTIR spectra were collected using Bruker ALPHA Infrared Spectrometer (Bruker, Billerica, MA). Thirty-two background scans of the empty chamber were taken followed by sixty-four sample scans of the various foam compositions. FTIR spectra were collected in absorption mode at a resolution of 4 cm<sup>-1</sup>. OPUS software (Bruker, Billerica,

MA) was utilized to subtract the background scans from the spectra, to conduct a baseline correction for IR beam scattering, and to normalize multiple spectra to one another. Each composition was measured three times, and one representative spectrum was chosen to display.



## CHAPTER III

### RESULTS<sup>3</sup>

#### 3.1 Results

For the majority of the testing, the most and least hydrophilic foam compositions (100HDIH40 and 100TMH60, respectively) were selected for characterization. Further classification of ebeam radiation effects was also carried out on 100HDIH60 foams (mid-range hydrophilicity) with multiple radiation doses (25 kGy and 40 kGy).

#### 3.2 Differential scanning calorimetry (DSC)

The results of the  $T_g$  analysis are shown in **Figure 3.1 A-D**. Thermal analysis revealed the largest change in dry  $T_g$  for nEtO-sterilized samples (39% change between control and sterilized sample). Ebeam and gamma sterilization produced consistent thermal behavior for all foam compositions and thermal tests. The thermograms of wet DSC measurements for 100HDIH40 foams (**Figure 3.1 D**) were difficult to read due to the proximity of the  $T_g$  to the recrystallization peak of water at 0 °C [50]. Thus, these results were not considered to be reliable indications of the effects of sterilization.

---

<sup>3</sup> Parts of this chapter are from “Effects of Sterilization on Shape Memory Polyurethane Embolic Foam Devices” by **R. Muschalek**, Nash L.D., Jones R, Hasan S.M., Keller B.K., Monroe M.B., Maitland D.J., which is under review by the Journal of Medical Devices.

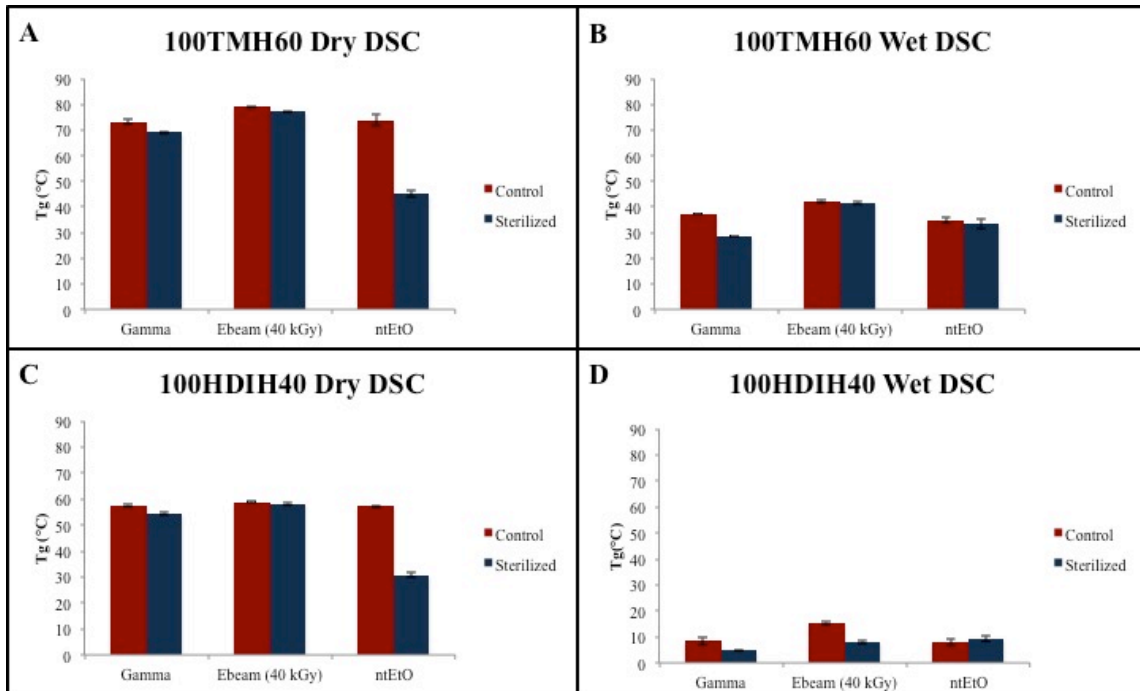


**Figure 3.1:**  $T_g$  measurements for the two foam compositions (A and B: 100TMH60; C and D: 100HDIH40) in dry (A and C) and wet (B and D) conditions.  $N = 3$ , average  $\pm$  standard deviation displayed.

### 3.3 Mechanical testing

**Figure 3.2** and **Figure 3.3** give the ultimate tensile strength (UTS) and strain at break, respectively, for each foam composition before and after sterilization. The large standard deviations arise from the intrinsic properties of the gas blown foam due to the inhomogeneous pore size and shape. No statistically significant differences in UTS or strain at break were seen following the three sterilization methods for either composition ( $p < 0.05$ ).

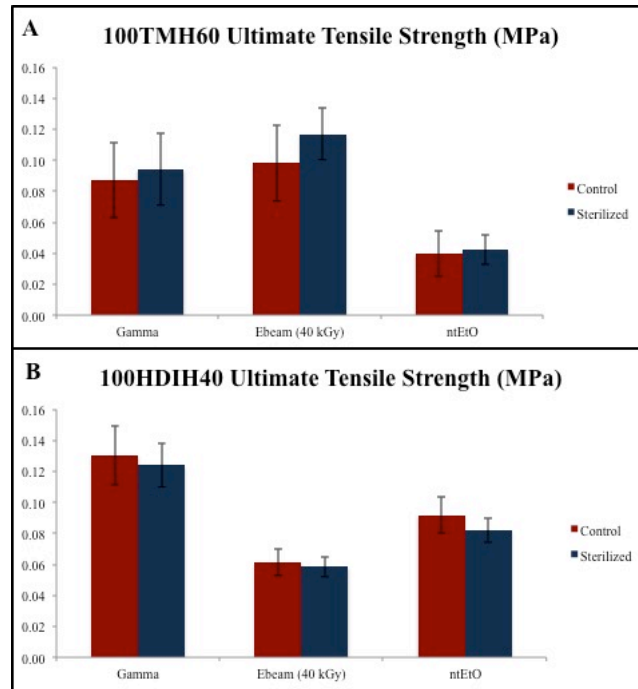


Figure 3.2: UTS of a) 100TMH60 and b) 100HDIH40 foams. No significant changes were seen before and after sterilization. N = 6, average  $\pm$  standard deviation displayed.

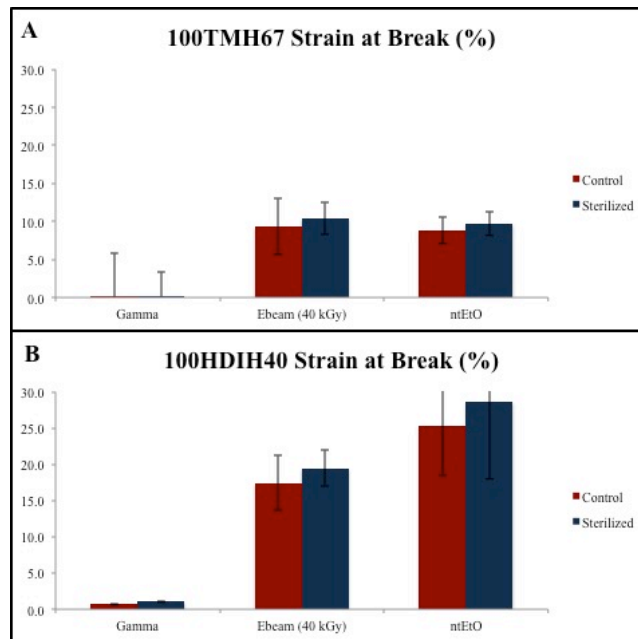


Figure 3.3: Strain at break of a) 100TMH60 and b) 100HDIH40 foams. No significant changes were seen before and after sterilization. N = 6, average  $\pm$  standard deviation displayed.

### 3.4 Crimp diameter

Yellowing of the gamma irradiated foam samples was observed, and at this point gamma was no longer pursued as a potential sterilization method due to hypothesized oxidative radicals that threatened to expedite bulk polymer degradation [51].

The results of the crimp diameter tests can be seen in Figure 3.4 and Tables 3.1 and 3.2. Some relaxation of the crimp is expected to occur, as seen in the control samples, which were left in a dry box for 1 week [52]. It should be noted that “N/A” for ntEtO in the 100HDIH40 samples indicates expansion beyond the constraints of the packaging that prevented imaging of final devices. Ebeam-sterilized cylinders expanded the least, indicating minimal process plasticization; thus, ebeam sterilization was chosen for further material classification following application of lower radiation dosage.

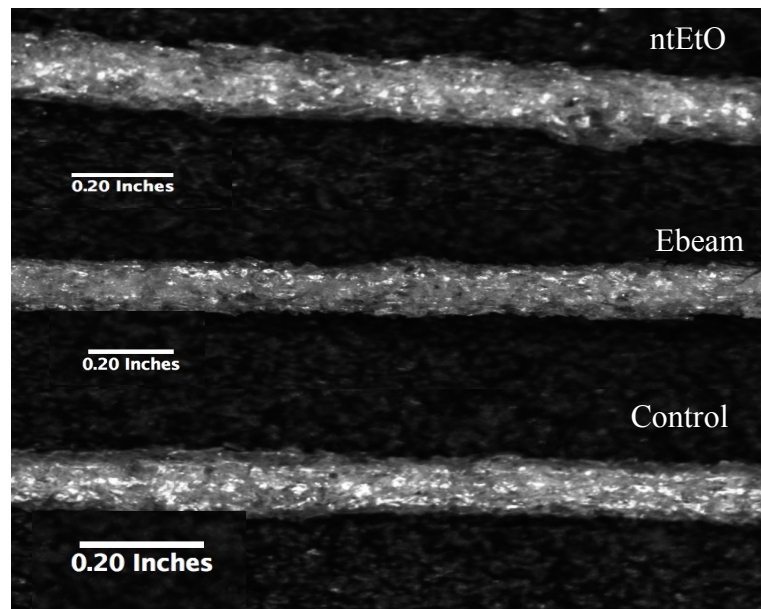


Figure 3.4: Cylindrically crimped 1 mm 100TMH60 foam after each method of sterilization. Images were taken with a Jenoptic microscope camera and analyzed using ImageJ software for average diameter

**Table 3.1: Cylindrical expansion of 100TMH60 foams following sterilization. N = 7, average  $\pm$  standard deviation displayed.**

<b>Sterilization Process</b>	<b>Initial Diameter (in)</b>	<b>Final Diameter (in)</b>	<b>Change in Diameter (in)</b>
<b>Control</b>	<b>0.0147 <math>\pm</math> 0.0008</b>	<b>0.0154 <math>\pm</math> 0.0007</b>	<b>0.0007</b>
<b>ntEtO</b>	<b>0.0145 <math>\pm</math> 0.0006</b>	<b>0.0163 <math>\pm</math> 0.0011</b>	<b>0.0018</b>
<b>Ebeam (25 kGy)</b>	<b>0.0145 <math>\pm</math> 0.0007</b>	<b>0.0158 <math>\pm</math> 0.0004</b>	<b>0.0013</b>

**Table 3.2: Cylindrical expansion of 100HDIH40 foams following sterilization. N = 3, average  $\pm$  standard deviation displayed.**

<b>Sterilization Process</b>	<b>Initial Diameter (in)</b>	<b>Final Diameter (in)</b>	<b>Change in Diameter (in)</b>
<b>Control</b>	<b>0.043 <math>\pm</math> 0.007</b>	<b>0.051 <math>\pm</math> 0.004</b>	<b>0.008</b>
<b>ntEtO</b>	<b>0.050 <math>\pm</math> 0.002</b>	<b>N/A</b>	<b>N/A</b>
<b>Ebeam (25 kGy)</b>	<b>0.041 <math>\pm</math> 0.005</b>	<b>0.041 <math>\pm</math> 0.001</b>	<b>0.000</b>

### 3.5 Unconstrained expansion

To more fully characterize ebeam sterilization, a second HDI foam composition (100HDIH60) in addition to the two previously characterized foams was exposed to two separate radiation doses (25 kGy and 40 kGy) and utilized in further material characterization. Unconstrained cylindrical expansion of ebeam-sterilized samples can be seen in **Figure 3.5 A-C**. Both of the HDI compositions (100HDIH40 and 100HDIH60) were fully expanded to their original diameters (8 mm for 100HDIH40 and

6 mm for 100HDIH60) within 10 minutes, while the TMDHI composition (100TMH60) did not achieve full recovery (1 mm) after 30 minutes of testing. The 100TMH60 foam exhibited faster expansion after exposure to radiation at both doses as compared to control (**Figure 3.5 A**), while the 100HDIH40 and 100HDIH60 both exhibited slower expansion with increasing radiation dose (**Figures 3.5 B, C**). The most likely cause of this discrepancy is the cylindrical size of the prototype devices. The 1 mm 100TMH60 devices are much smaller than the 8 and 6 mm 100HDIH40 and 100HDIH60 devices, respectively. This smaller diameter makes changes more difficult to observe, and the 100TMH60 foam expansion profiles are all within the same standard deviation range. Thus, using larger diameter samples and/or increasing the sample size would most likely produce more similar effects to those of the two larger diameter devices.

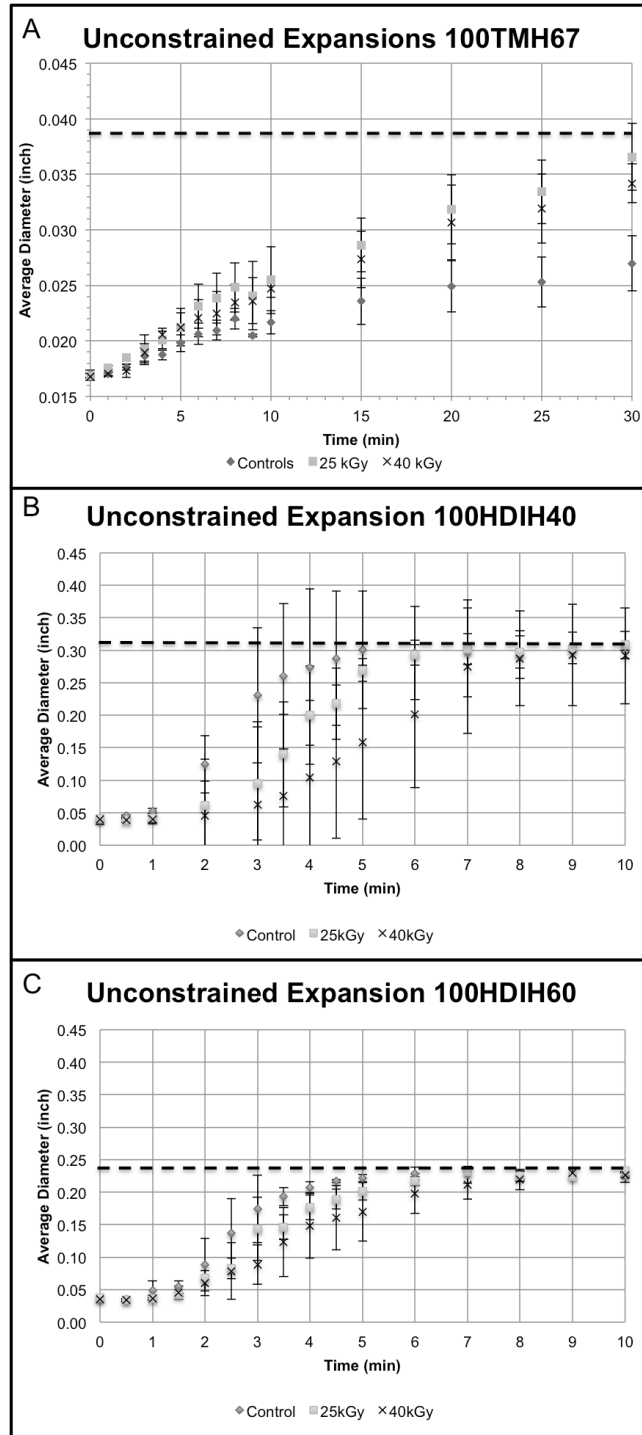


**Figure 3.5: Unconstrained expansion over time of exposure to 37°C water for ebeam sterilized (a) 100TMH60, (b) 100HDIH40, and (c) 100HDIH60 foams. N = 3, average ± standard deviation displayed. Dotted line indicates initial cut diameter dimensions.**

### 3.6 Fourier transform infrared (FTIR) spectroscopy

FTIR was used to detect any molecular differences that may have arisen during ebeam radiation on the three foam compositions. Selected FTIR spectral regions for the foam compositions can be seen in **Figure 3.6**. No noticeable differences were immediately detected between the control compositions and the ebeam sterilized compositions, indicating that radiation did not induce a *significant* molecular change in the foam samples. A potential expected change in spectra included oxidative degradation of the tertiary amine [42] which could be seen by an increase in the absorbance at 3400, indicating an increased –NH stretch post-sterilization [53]



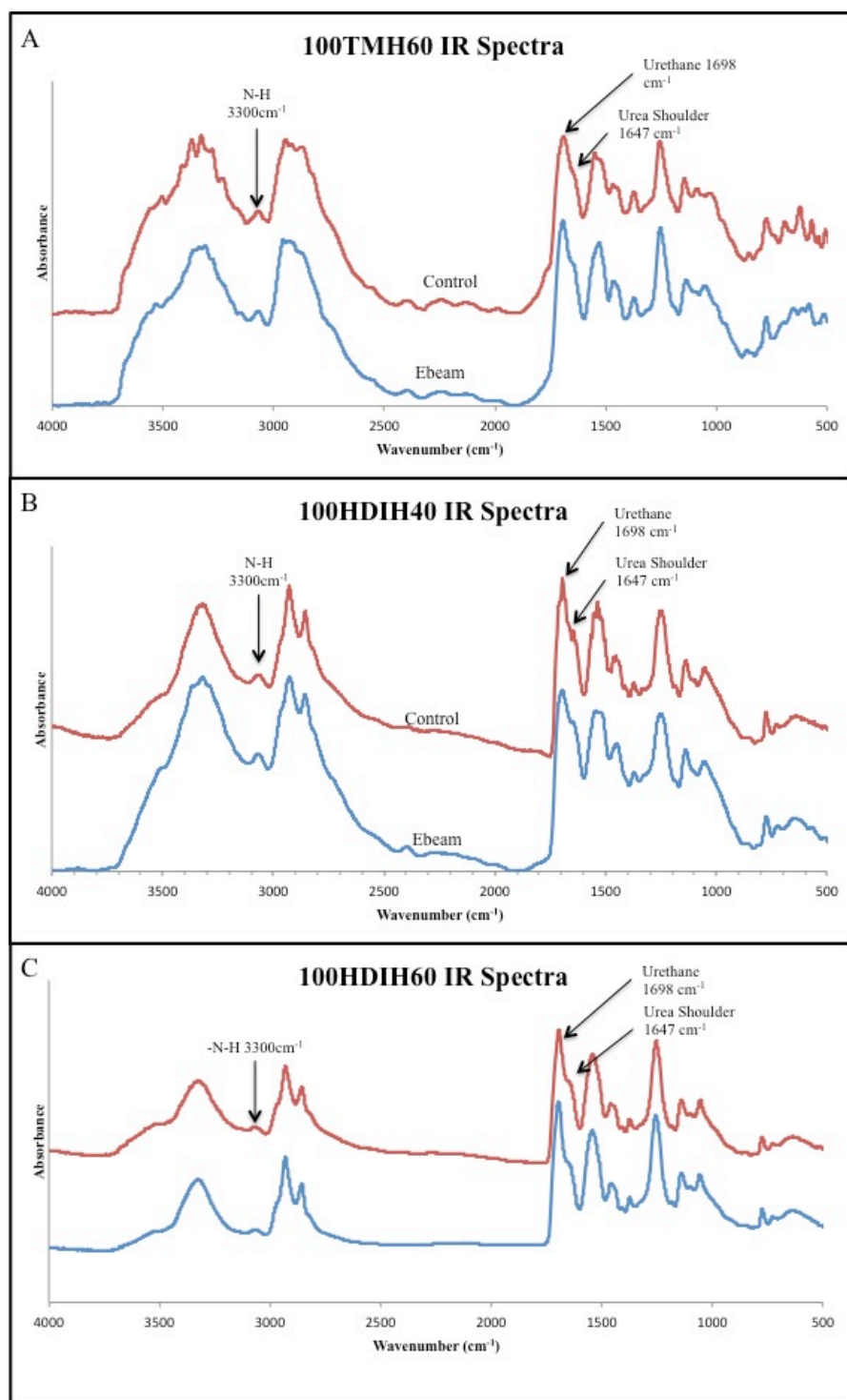


Figure 3.6: FTIR spectra of (a) 100TMH60, (b) 100HDIH40, and (c) 100HDIH60 before and after ebeam sterilization.

## CHAPTER IV

### CONCLUSIONS AND FUTURE WORK<sup>4</sup>

#### 4.1 Summary

SMP foams show promise for a variety of endovascular treatments because of their high shape recovery, porosity, and tunable transition temperature. Prior to this work, the effects of sterilization methods on polyurethane SMP foam properties SMP-based device functionality were unknown [39]. The FDA requires that all implantable medical devices undergo sterility assurance testing prior to submission of a premarket notification or premarket applications [54]. As a precursor to sterility assurance testing, one of many sterilization methods must be selected as the final sterilization method for SMP-based medical devices. To address this issue, in this work, SMP foam material properties were tested before and after three common sterilization methods: gamma radiation, nEtO, and ebeam radiation.

In Chapter II, the testing protocol was laid out for bulk material analysis as well as device functionality testing. All samples underwent DSC experiments to assess thermal changes induced in the foams due to sterilization processes. All samples also underwent mechanical tensile testing to failure to look at ultimate tensile strength and strain at break to see if any of the sterilization methods changed mechanical properties of the foam, which could have affected device functionality. NtEtO and ebeam samples

---

<sup>4</sup> Parts of this chapter are from “Effects of Sterilization on Shape Memory Polyurethane Embolic Foam Devices” by **R. Muschalek**, Nash L.D., Jones R, Hasan S.M., Keller B.K., Monroe M.B., Maitland D.J., which is under review by the Journal of Medical Devices.

continued in testing at this point with device prototypes being imaged before and after sterilization to see if the shape memory effect caused device expansion. Finally, the unconstrained expansion profiles and FTIR spectra of ebeam device prototypes were obtained to radiation altered shape memory properties or bulk molecular structure.

It was found that ntEtO-sterilized devices had significant moisture plasticization as compared to the two radiation sterilization methods tested. No statistically significant changes in mechanical properties were found for any sterilization method tested. Minimal device expansion due to sterilization method was seen for ebeam compared to ntEtO, which actually caused device failure in one of the foam compositions tested. Ebeam samples were tested for unconstrained expansion, and it was found that expansion time of the SMP increased with increasing radiation dose. Finally, ebeam samples were tested using FTIR to test for oxidative radicals that threaten the durability of the polymers long-term *in vivo* [51].

In conclusion, it was found that ebeam sterilized SMPs were the most functional after sterilization as compared to ntEtO sterilization and gamma radiation sterilization. The results from this study are critical to the clinical realization of SMP foam-based devices by identifying a reliable sterilization method for future pre-clinical safety and efficacy studies [38] [39].

## **4.2 Discussion**

The goal of this study was to identify and characterize a sterilization method that would not disrupt the functionality of a SMP foam-based medical device. In addition to

the tested methods, traditional ethylene oxide (EtO) is another common sterilization option for medical devices [41]. Due to the failure of the ntEtO-tested foam cylinders as noted by the large decrease in  $T_g$ , traditional EtO, which is a higher-heat, higher-humidity process, was removed as a potential sterilization method. Gamma radiation should be further investigated in future manuscripts due to the discrepancies that arose in packaging, which have significant impact on the potential for oxidative degradation [42] [46]. Ebeam radiation showed the most promise for SMP-based medical devices. Ebeam sterilization resulted in consistent properties between control foams and sterilized foams. Further characterization of electron beam sterilized foams indicated that no significant molecular changes occur during sterilization. NtEtO-sterilized foams appeared to have been moisture-plasticized during sterilization, as evidenced by a reduced  $T_g$  and increased diameter that prevented expansion characterization. This result is likely due to the relatively long exposure to the humidity (30%) in ntEtO in the moisture-permeable packaging. Ebeam-sterilized devices retained similar expansion profiles to controls with varied dosages and foam compositions. Volume expansion and working time are two of the most important functional considerations for SMP foam devices, as they define how effective a foam will be at shape-filling a defect site and how long a clinician has to deliver the device through the catheter before it expands and restricts delivery of the device, respectively. Maintenance of device functionality following sterilization is essential in successfully obtaining FDA clearance. Further characterization of electron beam sterilized foams indicated that no significant molecular changes occur during sterilization. Oxidation is a large concern for SMP foams, as it could alter long-term

stability and performance. Thus, a reduced potential of oxidation following ebeam sterilization is highly promising for SMP foam-based medical device development.

### **4.3 Challenges and future work**

Challenges of this work include the discrepancies seen in unconstrained expansion testing of the SMP foam cylinders. While the 100TMH60 foams appeared to expand more quickly with ebeam radiation, the 100HDIH40 and 100HDIH60 foams appeared to expand more slowly with radiation. It was hypothesized that two variables were confounding the final results of the expansions, namely: crosslinking rearrangement and surface oxidation. Further characterization of these two phenomena should be pursued because preliminary studies of each (using dynamic mechanical analysis or DMA, and attenuated total reflectance Fourier transform infrared spectroscopy or ATR-FITR) were inconclusive. A series with a single sample of each radiation dose in the DMA found that minimal crosslinking rearrangement was occurring. Preliminary ATR-FTIR data found that with ebeam radiation at high doses (60 kGy) and neat films packaged in ambient air, surface oxidation was occurring as seen by the generation of an amine-oxide peak at  $950\text{ cm}^{-1}$  [55].

The work that should be completed next is sterility assurance testing [54]. This work encompassed both radiation doses that are typically utilized for sterility testing, but a verification of sterilization is required for future device translation. The most common method of sterility assurance testing is called “Verification of Dose Maximum (VDmax) and entails a three step process of: (1) A bioburden test to quantify the viable

microorganisms on or in the product. This test is performed prior to any sterilization but after all other manufacturing steps including packaging, (2) An application of verification dose where the bioburden results are taken to a table from the standard (ISO 11137) to determine the proper verification dose. The verification dose is then applied to the required number of products. In the particular case of our SMP-based embolic devices the required radiation dose is most likely substantially lower than the doses tested herein because the research was attempting to assess the effects of the highest doses of radiation on the medical devices (3) A sterility test where irradiated products undergo a test of sterility including biological indicators. This takes into account a bacteriostasis/ Fugistasis test to demonstrate the lack of inhibition in the sterility test system and is required to validate sterility test.

Secondarily, gamma radiation sterilization could be re-visited as a potential for sterilization of SMP-based foam devices if correct packaging environments could be generated. There is still the concern of core wire heating due to gamma radiation, which could induce premature thermal actuation of the devices.

Finally, other researchers at the University of Texas at Dallas [38] suggest the use of 254 nm wavelength UV light for 120 minutes as another mode of plausible sterilization for SMP-based devices. This method should be investigated for any effects on polyurethane SMP foam expansion times.

## REFERENCES

- [1] Lendlein, A., and Kelch, S., 2002, "Shape-Memory Polymers," *Angewandte Chemie International Edition*, 41(12), pp. 2034-2057.
- [2] Landsman, T. L., Bush, R. L., Glowczwski, A., Horn, J., Jessen, S. L., Ungchusri, E., Diguette, K., Smith, H. R., Hasan, S. M., Nash, D., Clubb, F. J., and Maitland, D. J., 2016, "Design and verification of a shape memory polymer peripheral occlusion device," *Journal of the Mechanical Behavior of Biomedical Materials*, 63, pp. 195-206.
- [3] Ratner, B. D., Hoffman, A. S., Schoen, F. J., and Lemons, J. E., 2004, *Biomaterials Science: An Introduction To Materials in Medicine*, Academic press.
- [4] Small IV, W., Singhal, P., Wilson, T. S., and Maitland, D. J., 2010, "Biomedical applications of thermally activated shape memory polymers," *Journal of Materials Chemistry*, 20(17), pp. 3356-3366.
- [5] Baer, G., Wilson, T., Matthews, D., and Maitland, D., 2007, "Shape-memory behavior of thermally stimulated polyurethane for medical applications," *Journal of Applied Polymer Science*, 103(6), pp. 3882-3892.
- [6] Maitland, D. J., Small, W., Ortega, J. M., Buckley, P. R., Rodriguez, J., Hartman, J., and Wilson, T. S., 2007, "Prototype laser-activated shape memory polymer foam device for embolic treatment of aneurysms," *Journal of Biomedical Optics*, 12(3), pp. 030504-030504-030503.
- [7] Boyle, A., Weems, A., Hasan, S., Nash, L., Monroe, M., and Maitland, D., 2016, "Solvent stimulated actuation of polyurethane-based shape memory polymer foams using dimethyl sulfoxide and ethanol," *Smart Materials and Structures*, 25(7), p. 075014.
- [8] Singhal, P., Boyle, A., Brooks, M. L., Infanger, S., Letts, S., Small, W., Maitland, D. J., and Wilson, T. S., 2013, "Controlling the actuation rate of low-density shape-memory polymer foams in water," *Macromolecular Chemistry and Physics*, 214(11), pp. 1204-1214.
- [9] Singhal, P., Rodriguez, J. N., Small, W., Eagleston, S., Van de Water, J., Maitland, D. J., and Wilson, T. S., 2012, "Ultra low density and highly crosslinked biocompatible shape memory polyurethane foams," *Journal of Polymer Science Part B: Polymer Physics*, 50(10), pp. 724-737.

- [10] Hwang, W., Singhal, P., Miller, M. W., and Maitland, D. J., 2013, "In vitro study of transcatheter delivery of a shape memory polymer foam embolic device for treating cerebral aneurysms," *Journal of Medical Devices*, 7(2), p. 020932.
- [11] Boyle, A. J., Landsman, T. L., Wierzbicki, M. A., Nash, L. D., Hwang, W., Miller, M. W., Tuzun, E., Hasan, S. M., and Maitland, D. J., 2015, "In vitro and in vivo evaluation of a shape memory polymer foam-over-wire embolization device delivered in saccular aneurysm models," *Journal of Biomedical Materials Research Part B: Applied Biomaterials*(104B), pp. 1407–1415.
- [12] Metcalfe, A., Desfaits, A.-C., Salazkin, I., Yahia, L. H., Sokolowski, W. M., and Raymond, J., 2003, "Cold hibernated elastic memory foams for endovascular interventions," *Biomaterials*, 24(3), pp. 491-497.
- [13] Ratna, D., and Karger-Kocsis, J., 2008, "Recent advances in shape memory polymers and composites: a review," *Journal of Materials Science*, 43(1), pp. 254-269.
- [14] Rodriguez, J. N., Clubb, F. J., Wilson, T. S., Miller, M. W., Fossum, T. W., Hartman, J., Tuzun, E., Singhal, P., and Maitland, D. J., 2014, "In vivo response to an implanted shape memory polyurethane foam in a porcine aneurysm model," *Journal of Biomedical Materials Research Part A*, 102(5), pp. 1231-1242.
- [15] National Institute of Neurological Disorders and Stroke: National Institutes of Health, 2013, "Cerebral Aneurysms Fact Sheet."
- [16] Molyneux, A. J., Birks, J., Clarke, A., Sneade, M., and Kerr, R. S. C., "The durability of endovascular coiling versus neurosurgical clipping of ruptured cerebral aneurysms: 18 year follow-up of the UK cohort of the International Subarachnoid Aneurysm Trial (ISAT)," *The Lancet*, 385(9969), pp. 691-697.
- [17] Kumar, Abbas, Aster, 2014, "Robbins and Cotran Pathologic Basis of Disease," Saunders/Elsevier, Philadelphia, PA, pp. 344-345.
- [18] Humphrey, J. D., 2002, *Cardiovascular Solid Mechanics: Cells, Tissues, and Organs*, Springer, New York.
- [19] American Stroke Association, "What You Should Know About Cerebral Aneurysms,"  
[http://www.strokeassociation.org/STROKEORG/AboutStroke/TypesofStroke/HemorrhagicBleeds/What-You-Should-Know-About-Cerebral-Aneurysms\\_UCM\\_310103\\_Article.jsp](http://www.strokeassociation.org/STROKEORG/AboutStroke/TypesofStroke/HemorrhagicBleeds/What-You-Should-Know-About-Cerebral-Aneurysms_UCM_310103_Article.jsp).



- [20] Bederson, J. B., et al. , "Guidelines for the management of aneurysmal subarachnoid hemorrhage a statement for healthcare professionals from a special Writing Group of the Stroke Council, American Heart Association," *Stroke*, 40(3), pp. 994-1025.
- [21] The Brain Aneurysm Foundation, 2017, "Clipping," <http://www.bafound.org/about-brain-aneurysms/treatment/treatment-options/clipping/>.
- [22] The New Jersey Comprehensive Stroke Center at University Hospital, 2013, "Treating Acute Hemorrhagic Stroke," <http://www.uhnj.org/stroke/hemorrhagic.htm>.
- [23] Zuccarello, M., Ringer, A., 2016, "Aneurysm Surgery: Clipping," <http://www.mayfieldclinic.com/PDF/PE-Clipping.pdf>.
- [24] Andrew Ringer, 2016, "Aneurysm embolization: coiling," <http://www.mayfieldclinic.com/PDF/PE-Coiling.pdf>.
- [25] Pandey AS, K. C., Rosenwasser RH, Veznedaroglu E, 2007, "Endovascular coil embolization of ruptured and unruptured posterior circulation aneurysms: review of a 10-year experience.," *Neurosurgery*, 60(4), pp. 626-636.
- [26] Szikora, I., et al., 2006, "Histopathologic evaluation of aneurysms treated with Guglielmi detachable coils or matrix detachable microcoils," *American Journal of Neuroradiology* 27(2), pp. 283-288.
- [27] Ortega, J., Maitland, D.J., Wilson, T.S., Tsai, W. Savas, O., Saloner, D., 2007, "Vascular dynamics of a shape memory polymer foam aneurysm treatment technique," *Annals of Biomedical Engineering*, 35(11), pp. 1870-1884.
- [28] Kallmes, D. F., Fujiwara, N.H., Yuen, D., Dai, D., Li, S.q, 2003, "A collagen-based coil for embolization of saccular aneurysms in a New Zealand white rabbit model," *American Journal of Neuroradiology*, 24, pp. 591-596.
- [29] McDougall, C. G., Claiborne Johnston, S., Gholkar, A., Barnwell, S.L., Vazquez Suarez, J.C., Masso Romero, J., Chaloupka, J.C., Bonafe, A., Wakhloo, A.K., Tampieri, D., Dowd, C.F., Fox, A.J., Imm, S.J., Carroll, K., , 2014, "Bioactive versus bare platinum coils in the treatment of intracranial aneurysms: The MAPS (Matrix and Platinum Science) Trial," *American Journal of Neuroradiology*, 35, pp. 935-942.
- [30] Horn, J., Hwang, W., Jessen, S. L., Keller, B. K., Miller, M. W., Tuzun, E., Hartman, J., Clubb, F. J., and Maitland, D. J., 2016, "Comparison of shape memory

polymer foam versus bare metal coil treatments in an in vivo porcine sidewall aneurysm model," *Journal of Biomedical Materials Research Part B: Applied Biomaterials*, pp. n/a-n/a.

[31] Horowitz, M., Samsun, D., Purdy, P., 1997, "Does electrothrombosis occur immediately after embolization of an aneurysm with Guglielmi detachable coils?," *American Journal of Neuroradiology*, 18, pp. 510-513.

[32] Landsman, T., 2016, "Design and verification of shape memory polymer embolization devices for peripheral indications," Doctor of Philosophy Texas A&M University.

[33] Small IV, W., Wilson, T. S., Benett, W. J., Loge, J. M., and Maitland, D. J., 2005, "Laser-activated shape memory polymer intravascular thrombectomy device," *Opt. Express*, 13(20), pp. 8204-8213.

[34] Kotzar, G., Freas, M., Abel, P., Fleischman, A., Roy, S., Zorman, C., Moran, J. M., and Melzak, J., 2002, "Evaluation of MEMS materials of construction for implantable medical devices," *Biomaterials*, 23(13), pp. 2737-2750.

[35] Rutala, W. A., Weber, D. J., and Control, C. f. D., 2008, *Guideline for disinfection and sterilization in healthcare facilities, 2008*, Centers for Disease Control (US).

[36] (ISO), I. S. O., 2009, "Biological evaluation of medical devices -- Part 1: Evaluation and testing within a risk management process," 10993-1.

[37] (ANSI), A. N. S. I., 2013, "Sterilization of health care products — Radiation —Part 2: Establishing the sterilization dose " 11137-2.

[38] Ecker, M. D., Vindhya; Shoffstall, Andrew J.; Mahmood, Samsuddin F.; Joshi-Imre, Alexandra; Frewin, Christopher L.; Ware, Taylor H.; Capadona, Jeffrey R.; Pancrazio, Joseph J.; Voit, Walter E., 2016, "Sterilization of thiol-ene/acrylate based shape memory polymers for biomedical applications," *Macromolecular Materials and Engineering*, pp. 1439-2054.

[39] Wong, Y., Kong, J., Widjaja, L. K., and Venkatraman, S. S., 2014, "Biomedical applications of shape-memory polymers: how practically useful are they?," *Science China Chemistry*, 57(4), pp. 476-489.

- [40] Wilson, T., Bearinger, J., Herberg, J., Marion, J., Wright, W., Evans, C., and Maitland, D., 2007, "Shape memory polymers based on uniform aliphatic urethane networks," *Journal of Applied Polymer Science*, 106(1), pp. 540-551.
- [41] Mendes, G. C., Brandao, T. R., and Silva, C. L., 2007, "Ethylene oxide sterilization of medical devices: a review," *American Journal of Infection Control*, 35(9), pp. 574-581.
- [42] Premnath, V., Harris, W. H., Jasty, M., and Merrill, E. W., 1996, "Gamma sterilization of UHMWPE articular implants: an analysis of the oxidation problem," *Biomaterials*, 17(18), pp. 1741-1753.
- [43] Smith, R., and Young, J., 1968, "Simplified gas sterilization: A new answer for an old problem," *British Journal of Anaesthesia*, 40(11), pp. 909-915.
- [44] Martin, J., 2012, "Understanding Gamma Sterilization," <http://www.biopharminternational.com/understanding-gamma-sterilization>.
- [45] Woo, L., and Sandford, C. L., 2002, "Comparison of electron beam irradiation with gamma processing for medical packaging materials," *Radiation Physics and Chemistry*, 63(3-6), pp. 845-850.
- [46] Silindir, M., and Ozer, A., 2009, "Sterilization methods and the comparison of e-beam sterilization with gamma radiation sterilization," *FABAD J Pharm Sci*, 34(34), pp. 43-53.
- [47] Allen, J. T., Calhoun, R., Helm, J., Kruger, S., Lee, C., Mendonsa, R., Meyer, S., Pageau, G., Shaffer, H., Whitham, K., Williams, C. B., and Farrell, J. P., 1995, "Proceedings of the 29th international meeting on radiation processing: a fully integrated 10 MeV electron beam sterilization system," *Radiation Physics and Chemistry*, 46(4), pp. 457-460.
- [48] Hasan, S. M., Harmon, G., Zhou, F., Raymond, J. E., Gustafson, T. P., Wilson, T. S., and Maitland, D. J., 2016, "Tungsten-loaded SMP foam nanocomposites with inherent radiopacity and tunable thermo-mechanical properties," *Polymers for Advanced Technologies*, 27(2), pp. 195-203.
- [49] Hasan SM, T. R., Emery H, Nathan AL, Weems AC, Zhou F, Wilson TS, Maitland DJ 2016, "Modification of shape memory polymer foams using tungsten, aluminum oxide, and silicon dioxide nanoparticles," *RSC Advances*, 6, pp. 918 – 927.

[50] ZH Ping, Q. N., SM Chen, JQ Zhou, YD Ding, 2001, "States of water in different hydrophilic polymers- DSC and FTIR studies," *Polymer*, 42, pp. 8461-8467.

[51] AC Weems, K. W., KL Wooley, DJ Maitland., "Degradation of shape memory polymers: examination of highly porous, thermoset polyurethanes," *Proceedings from American Chemical Society (ACS) National Meeting*.

[52] Qi, H. J., and Boyce, M. C., 2005, "Stress-strain behavior of thermoplastic polyurethanes," *Mechanics of Materials*, 37(8), pp. 817-839.

[53] Coates, J., 2006, "Interpretation of Infrared Spectra, A Practical Approach," *Encyclopedia of Analytical Chemistry*, John Wiley & Sons, Ltd, pp. 10815–10837.

[54] Center for Devices and Radiological Health, 2016, "Submission and Review of Sterility Information in Premarket Notification (510(k)) Submissions for Devices Labeled as Sterile Guidance for Industry and Food and Drug Administration Staff," F. a. D. Administration, ed.

[55] Segneanu, A. E., Gozescu, I., Dabici, A., Sfirloaga, P., and Szabadai, Z., 2012, "Organic compounds FT-IR spectroscopy," Edited by Jamal Uddin, p. 145.